Journal of the American Ceramic Society

RESEARCH ARTICLE OPEN ACCESS

3D Printing Polymer Derived SiC/SiOC(N) Ceramic Matrix Composites From Replica of SiC/Polyurethane Cellular Structures

Rajat Chaudhary[1,2] | Jochebed Zyambo[1] | Sereno Sacchet[3] | Luca Fambri[3] | Mattia Biesuz[1,2] | Gian Domenico Sorarù[1,2]

[1]Glass & Ceramics Lab, Department of Industrial Engineering University of Trento, Trento, Italy | [2]Consorzio Interuniversitario Nazionale per la Scienza e Tecnologia dei Materiali, Firenze, Italy | [3]Polymer & Composite Lab Department of Industrial Engineering University of Trento, Trento, Italy

Correspondence: Rajat Chaudhary (rajat.chaudhary@unitn.it)

Received: 21 October 2025 | **Revised:** 21 January 2026 | **Accepted:** 23 February 2026

Keywords: composites | manufacturing | polymer precursor | silicon carbide | silicon oxycarbide

ABSTRACT

Cellular SiC/thermoplastic polyurethane (TPU) components were printed via fused filament fabrication and impregnated with a commercial polysilazane. The pyrolysis process in an inert atmosphere converts the structure into a ceramic-matrix composite through the polymer-derived ceramics (PDCs) route. Eventually, cellular components constituted by an amorphous SiOC(N) matrix with a dispersed SiC phase were obtained. The structural evolution was investigated via infrared spectroscopy, while the microstructure was studied via scanning electron microscopy. Properties like Vickers hardness, skeletal density, and compressive strength have been measured. The results indicate that the process allows the preparation of cellular structures with composite ceramic struts and a homogeneously distributed particulate reinforcing phase. The process opens new opportunities for the 3D-printing of PDCs as the dispersed phase can tailor the pyrolysis shrinkage, improve the mechanical properties of the component, and, if properly tailored, introduce new functionalities.

1 | Introduction

Cellular ceramic structures (CCSs), fabricated using additive manufacturing (AM), also known as 3D printing, are the focus of extensive research activities. Numerous comprehensive reviews on this topic are available in the literature [1, 2]. In terms of composition, CCSs have been developed from a variety of materials, including pure oxides (e.g., Al_2O_3, ZrO_2), ceramic composites (e.g., Al_2O_3/ZrO_2), and carbides or nitrides (e.g., SiC, Si_3N_4). These materials are selected based on the desired mechanical, thermal, or chemical properties of the final components.

The applications of CCSs are broad and diverse, spanning several high-performance domains. In the energy sector, they can be used as heat exchangers; in chemical engineering, as catalyst supports; in biomedical fields, as scaffolds for bone regeneration; and in aerospace or automotive industries, as lightweight components capable of withstanding high temperatures.

Silicon-based ceramic structures can be prepared via the polymer-derived ceramic (PDC) route, using Si-containing polymers such as polycarbosilanes, polysilazanes, or polysiloxanes. These precursors lead to the formation of silicon carbide (SiC), silicon carbonitride (SiCN), and silicon oxycarbide (SiOC) [3–5]. Typically, 3D printing of PDCs is performed either by direct ink writing (DIW) of a suspension containing a liquid pre-ceramic polymer, or by VAT photopolymerization of a pre-ceramic polymer with vinyl functionalities.

A more recent approach to AM with pre-ceramic polymers was developed in our laboratory and involves 3D printing a thermoplastic polyurethane (TPU) lattice using fused filament fabrication (FFF), which is then: (i) impregnated with a polysilazane, (ii) crosslinked, and (iii) pyrolyzed in an inert atmosphere to yield a SiOC(N) lattice [6]. This method, which falls under the broader category of replica techniques, offers several advantages:

i. The final ceramic lattice exhibits dense struts, suggesting that the pre-ceramic polymer diffuses into the TPU matrix rather than merely coating the surface [7], which would otherwise result in hollow struts after pyrolysis;
ii. the process utilizes simple and widely available equipment, such as FFF printers, avoiding the need for more complex setups required for photopolymerization;
iii. it eliminates the need for precise control over ink rheology, which is often critical in DIW processes.

SiOC(N) cellular structures fabricated with this replica method have shown excellent performance as bone regeneration scaffolds [8] as well as high temperature stability [6].

In this study, we extend this innovative replica method for the fabrication of ceramic composite structures (CCSs) featuring SiC/SiOC(N) composite struts. The core concept is to replace the conventional use of a neat TPU filament for printing the sacrificial lattice with a composite SiC/TPU filament, in which SiC particles are dispersed within a TPU matrix. Following 3D printing, the printed SiC/TPU composite lattice is infiltrated with a polysilazane precursor and subsequently pyrolyzed. This process is expected to yield a ceramic replica not only of the overall lattice architecture but also of the initial SiC/TPU microstructure, in which SiC particles are embedded within a continuous SiOC(N) matrix.

2 | Experimental Details

2.1 | Sample Preparation

NinjaFlex, a commercial TPU filament, was purchased from NinjaTek (Lititz, PA, USA), and β-SiC powders (2 μm, Norton, Lillesand, Norway) were used as filler. A commercial polysilazane (Durazane 1800, Merck, Darmstadt, Germany) was used as preceramic polymer for the infiltration process. The polymer crosslinking was catalyzed using a platinum divinyltetramethyldisiloxane complex, Pt 2% in xylene (CAS number: 68478-92-2, Sigma-Aldrich, St. Louis, MO, USA).

The Ninjaflex TPU and the SiC powders were compounded using a Thermo Haake Rheomix 600 (Thermo Fisher Scientific, USA) equipped with counter-rotating screws at a constant rotation of 50 rpm at 175°C. First, the neat TPU was inserted in the chamber (45 cm^3) and compounded for 5 min, and subsequently the SiC powder was gradually added, and the blend was compounded for 10 min to homogeneously distribute the filler. Accordingly, compounds SiC/TPU 15/85, 20/80 and 25/75 wt% were prepared.

The cooled blend was machined using an RN 166/1 granulator equipped with a 3 mm sieve to obtain granules. These granules were extruded with a Thermo Haake Rheomex (Thermo Fisher Scientific, USA) equipped with co-rotating twin screws (diameter of 16 mm and length to diameter ratio of 25). The screw rotation was set at 5 rpm, and a temperature profile from 140°C to 180°C was imposed into the cylinder. The nozzle of the extruder had a diameter of 1.8 mm, and abundant air cooling was applied before collecting the filament, regulating the collection speed to compensate the pronounced filament swelling and obtaining a final diameter of ~1.75 mm.

Samples with dimensions of approximately 15 × 15 × 15 mm^3 (for compression tests) and 15 × 15 × 5 mm^3 (for all other characterizations) were designed in Fusion 360 CAD software. An open-source Lulzbot TAZ 6 (Fargo Additive Manufacturing 3D) printer was used to print samples using TPU and SiC/TPU filament (1.75 mm diameter). A 0.25 mm nozzle was used for all prints. The slicing software CURA (open-source) was employed to define the following printing parameters: layer thickness (200 μm), wall thickness (300 μm), infill pattern (grid), infill gap (2 mm), printing speed (7 mm/s), printing temperature (225°C), and bed temperature (50°C).

The printed samples were impregnated with the polysilazane (Durazane 1800) using a two-step process: First, they were immersed in acetone containing the Pt catalyst, and then they were transferred and immersed in the liquid polysilazane for 5 min. The impregnated samples were then dried in air at room temperature for 48 h. Details of this procedure can be found in the literature [7].

An alumina tube furnace (GERO tube furnace) was adopted to perform the pyrolysis in a nitrogen atmosphere (100 cc/min). The temperature was increased at 2°C/min up to 160°C with a 3-h isothermal hold to ensure further crosslinking of the polysilazane. Then, a slower ramp of 0.5°C/min was used to reach 800°C, minimizing warping or cracking during ceramization. Subsequently, a 2°C/min ramp was applied up to 1200°C, with a 10 min isothermal hold, followed by furnace cooling to room temperature.

2.2 | Characterization

For each characterization technique and composition—neat SiOC, 15 wt% SiC, 20 wt% SiC, and 25 wt% SiC—a total of five samples were tested to ensure reproducibility and statistical reliability.

Tensile tests were performed on all SiC/TPU filament compositions prior to 3D printing to evaluate the effect of ceramic particle incorporation on filament mechanical performance. Tests were carried out on an Instron Universal Testing Machine (model 5969) equipped with grips designed for filament geometry to ensure accurate measurements and load cell of 1 kN. A gauge length of 100 mm and a strain rate of 10 mm/min were applied.

Impregnation of the cellular structures with Durazane 1800 was monitored by measuring the resulting weight and volume increases. Pyrolysis behavior was evaluated by measuring weight loss after treatment at 1200°C for 2 h.

TABLE 1 | Mechanical characterization data of the SiC/TPU filaments.

SiC content	Young's modulus	Max tensile stress	Elongation at break
(wt%)	(MPa) ± SD	(MPa) ± SD	(mm/mm) ± SD
0	15 ± 1.0	34 ± 1.8	4 ± 0.1
15	13 ± 2.4	36 ± 5.3	7 ± 0.2
20	16 ± 0.7	32 ± 0.4	7 ± 0.3
25	28 ± 1.0	27 ± 0.2	6 ± 0.1

The ceramic cellular structures obtained at 1200°C were characterized by geometrical and skeletal density measurements using a helium pycnometer (Ultrapyc 3000, Anton Paar, Rivoli, TO, Italy). Microstructural observations were performed by SEM on both fracture surfaces and polished cross-sections (diamond paste). Prior to imaging, samples were coated with a thin Au/Pd film. The chemical structure was analyzed by Fourier transform infrared spectroscopy (FT-IR, PerkinElmer Spectrum One) in attenuated total reflectance mode. Vickers hardness (HV) was determined using an FM-310 microhardness tester with a load of 200 gf.

Compression tests were performed on ceramized cubic samples approximately 13 × 13 × 13 mm^3. The top and bottom surfaces were polished to ensure flat, parallel faces prior to testing. For each composition, five samples were tested. Compression tests were conducted on an MTS universal testing machine fitted with a 70 kN load cell at a constant crosshead speed of 0.8 mm/s.

3 | Results

3.1 | Fabrication of the Composite Filaments, Polymeric Cellular Structures and Impregnation

Table 1 shows the mechanical properties of the as-prepared SiC/TPU filament.

The results show that adding 15 wt% of SiC powder to neat TPU decreases the elastic modulus, while increasing the tensile strength and elongation at break. However, when the SiC content is further increased from 15 to 25 wt%, the stiffness increases (as indicated by a higher elastic modulus), accompanied by a slight reduction in tensile strength. The elongation at break remains constant or decreases slightly with higher SiC content. The relatively low standard deviations indicate good repeatability and consistent filament quality across batches, supporting the reliability of the extrusion process. Cellular structures were easily printed with all the SiC/TPU filament compositions as shown in Figure 1.

Impregnation of the polymeric components with liquid polysilazane led to an increase in both volume and weight (Table 2 and Figure 2).

Neat TPU samples exhibit a 57% ± 1.9% increase in volume and a 71% ± 4.4% increase in weight. The incorporation of 15 wt% SiC powder further enhances the swelling ratio and mass uptake to

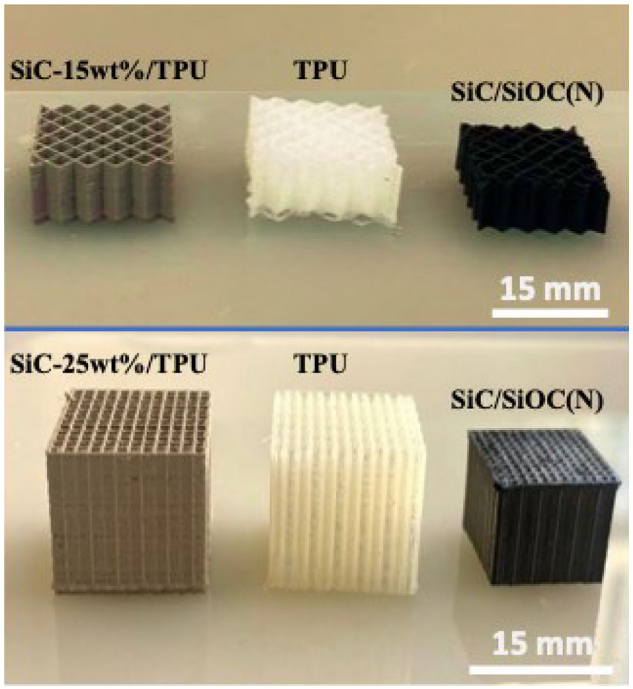

FIGURE 1 | Examples of cellular components printed with commercial Ninjaflex (neat TPU) filament; SiC–15 wt%/TPU filament; SiC–25 wt%/TPU filament, and the corresponding SiC/SiOC(N) structures after pyrolysis at 1200°C in N_2 flow. Cubic samples were used in compression tests.

65% and 77%, respectively. However, with higher SiC loadings, the trend reverses, and both swelling and mass uptake decrease with increasing SiC content. Specifically, the samples exhibit a progressive reduction in both volume expansion and weight gain as the SiC content increases.

Since swelling is mainly attributed to the diffusion and entrapment of Durazane 1800 within the TPU chains, the infiltration efficiency, that is, volume swelling and mass uptake in SiC/TPU composites is expected to decrease as the SiC content increases.

The ceramic yield after pyrolysis increases from 47% ± 3.0%, for the neat TPU samples, and stabilizes around 57%–58% for the SiC-containing samples. This result is consistent with expectations, as the SiC particles do not undergo weight loss during pyrolysis and therefore contribute to the increased ceramic yield of the composites.

3.2 | Characterization of the Ceramic Structures

The impregnated SiC/TPU 3D-printed structures were converted into SiC/SiOC(N) composites by pyrolysis at 1200°C in N_2 (Figure 1). The ceramic microstructure was examined by SEM on fracture surfaces (Figure 3). Neat TPU impregnated with polysilazane produced dense, featureless SiOC(N) struts, typical of glassy materials (Figure 3A and inset) in agreement with a previous work [6]. The microstructure of the SiC/SiOC(N) composites is shown in Figure 3B–D. The SiC particles are homogeneously distributed within the SiOC(N) ceramic matrix, confirming the success of the new composite synthesis approach.

TABLE 2 | Volume swelling and weight gain after impregnation and ceramic yield after pyrolysis.

Sample	Impregnation		Pyrolysis
	Volume swelling (%) ± SD	Weight gain (%) ± SD	Ceramic yield (%) ± SD
Neat TPU	57 ± 1.9	71 ± 4.4	47 ± 3.0
15% SiC	65 ± 2.5	78 ± 10.2	58 ± 2.2
20% SiC	58 ± 9.0	65 ± 6.6	57 ± 1.2
25% SiC	52 ± 2.4	63 ± 3.1	58 ± 3.0

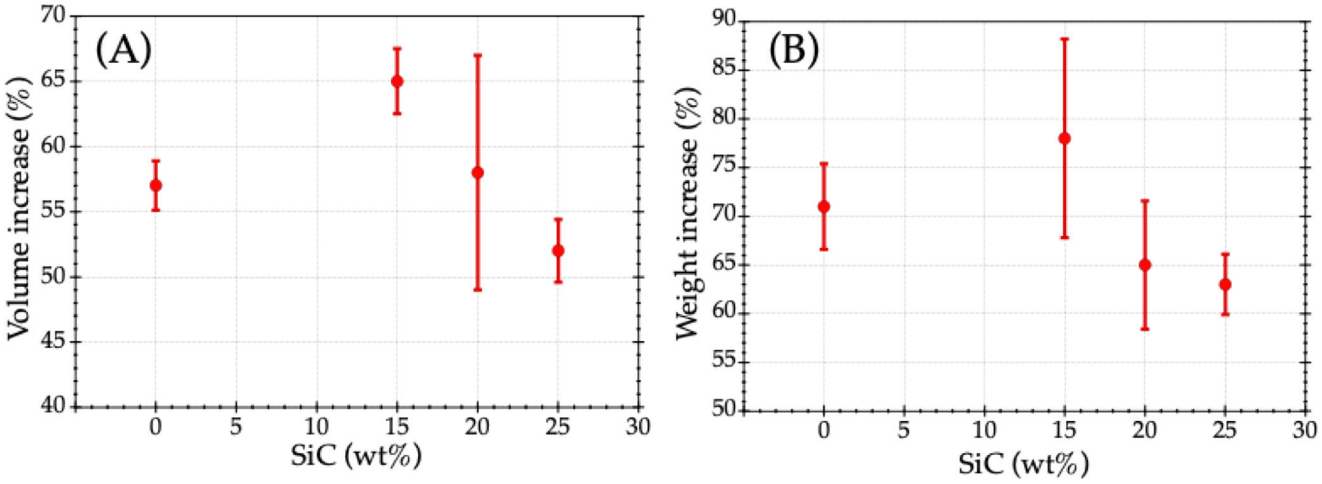

FIGURE 2 | Volume increase (A) and weight gain (B) upon impregnation as a function of SiC content in the SiC/TPU filament.

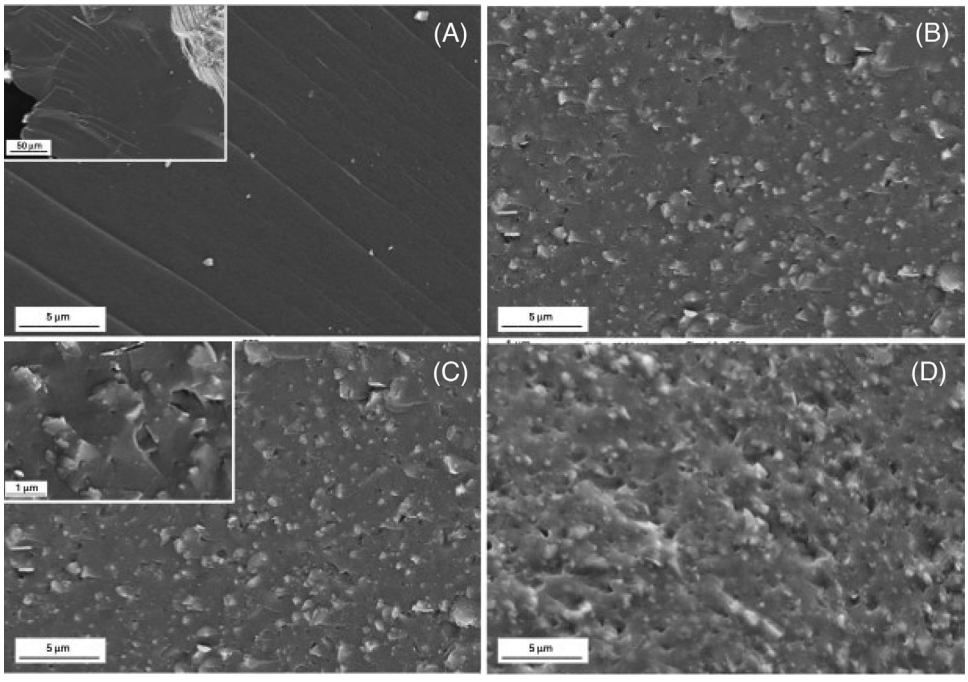

FIGURE 3 | SEM fracture surfaces of samples pyrolyzed at 1200°C. (A) Neat TPU (inset: lower-magnification image showing the formation of a dense strut); (B) SiC–15 wt%/TPU; (C) SiC–20 wt%/TPU (inset: higher-magnification image showing the intergranular fracture path); and (D) SiC–25 wt%/TPU.

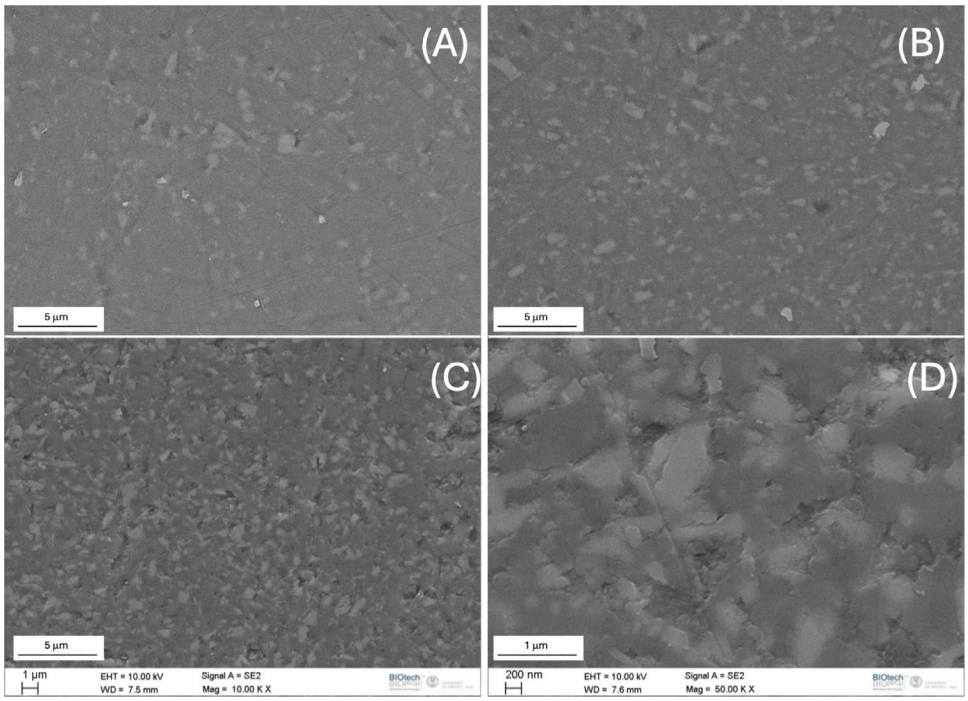

FIGURE 4 | SEM polished surfaces of samples pyrolyzed at 1200°C. (A) SiC–15 wt%/TPU; (B) SiC–20 wt%/TPU; (C) and (D) SiC–25 wt%/TPU.

Moreover, the presence, in the final composite, of the SiC particles was confirmed by EDS (see Figure S2). SEM did not clearly reveal residual porosity; however, it indicated an intergranular fracture path at the SiC/SiOC(N) interface (see inset, Figure 3C).

SEM images of polished surfaces of the SiC/SiOC(N) ceramics are shown in Figure 4. The homogeneous dispersion of SiC particles within the SiOC(N) matrix is evident. The surface of the SiC–25 wt%/TPU sample (Figure 4C,D) appears relatively rough; however, the observed voids correspond to SiC grain pull-out rather than residual porosity.

FT-IR spectra of the ceramic samples are shown in Figure 5. The pure SiOC(N) sample exhibits bands of the Si–O network at: 1060 cm^{-1} (Si–O stretching) and 470 cm^{-1} (Si–O–Si rocking). The spectra of the SiC/SiOC(N) composites display an additional peak at 840 cm^{-1}, attributed to Si–C stretching, whose intensity increases with SiC content. Interestingly, compared with the SiOC(N) spectrum, the FT-IR spectra of the SiC/SiOC(N) composites also exhibit bands at 1560 and 1420 cm^{-1}, attributed to C = C bonds and C–H vibrations of a carbonaceous phase [9–11]. This suggests that the presence of SiC particles during the pyrolysis of the polysilazane-impregnated TPU either promotes the formation of a free-carbon phase or increases its defectiveness, or possibly both.

Density values are reported in Table 3 and in Figure 6.

The skeletal density increases with the increase of the volume fraction of SiC particles in the composites and reaches a value of 2.40 ±0.02 g cm^{-3} for ≈20 vol% of SiC particles. The estimated density values are in good agreement with the measured ones.

HV was measured using a load of 200 gf (Figure 7), and the values increase linearly with the volume fraction of SiC, reaching 850

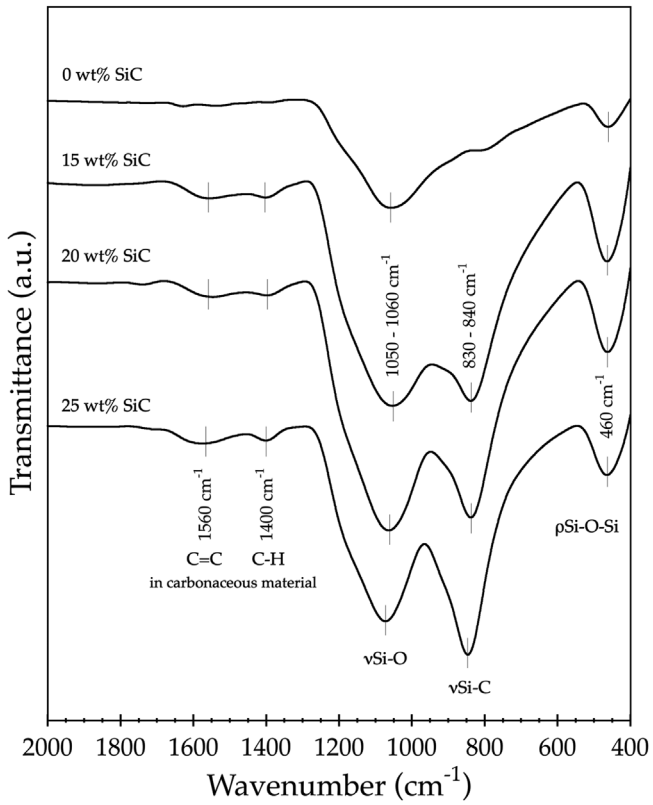

FIGURE 5 | FT-IR spectra of the of the ceramic samples.

± 25 HV at 20.5 Vol%. At this load (200 gf), no radial cracks originated from the impression corners (Figure 7). However, some cracks resembling cone cracks, like those that develop in silica glass, were observed. This is consistent with previous studies reporting that SiOC glasses pyrolyzed at 1200°C develop cone

TABLE 3 | Skeletal (measured and calculated) and geometrical density of the ceramic cellular samples. The volume percent (Vol-SiC) of the SiC phase in the ceramic composite is also reported. A detailed description of how the skeletal density and the SiC volume percent are calculated is reported in the Supporting Information (Table SI_1).

	Skeletal density (g cm^{-3})		Geometrical density (g cm^{-3})	Vol-SiC (%)
Sample	**Measured ± SD**	**Calculated**	**Measured ± SD**	**Calculated**
SiC-0/TPU	2.17 ± 0.2		0.39 ± 0.3	0
SiC-15/TPU	2.25 ± 0.2	2.28	0.49 ± 0.2	10.3
SiC-20/TPU	2.36 ± 0.2	2.33	0.49 ± 0.2	15.4
SiC-25/TPU	2.40 ± 0.2	2.37	0.50 ± 0.3	19.6

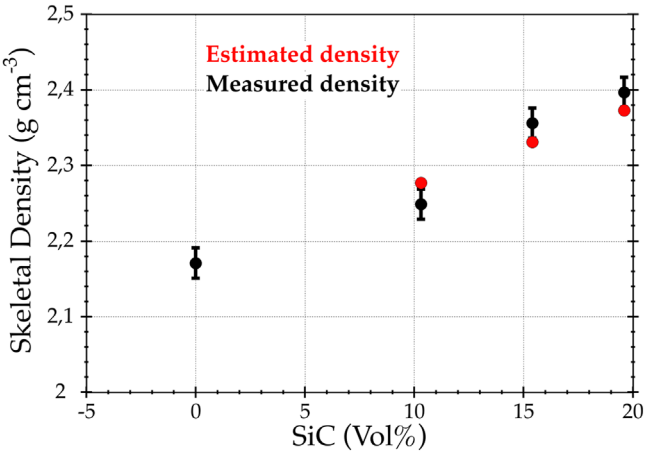

FIGURE 6 | Skeletal density values—measured and estimated—for the ceramic samples. Note that in this plot, the density is reported as a function of the volume fraction of SiC particles in the ceramic composite rather than the wt% of SiC in the starting SiC/TPU.

cracks, while only increasing the pyrolysis temperature above 1200°C leads to the formation of radial cracks at the impression corners [12, 13]. Any attempt to increase the indentation load to force the development of radial cracks failed up to 1000 gf.

Cubic ceramic samples shown in Figure 1 were tested in compression, and the results are reported in Figure 8A. Although it is difficult to observe a clear improvement in compressive stress when the minimum amount of SiC is added, there is nonetheless a noticeable increase in compressive strength when comparing the three samples containing SiC. Indeed, with the introduction of SiC, a gradual improvement in compressive strength is observed, reaching ≈50 MPa at higher SiC loadings of 19.6 Vol%. Compared to other types of ceramic structures (Figure 8B), including SiOC ceramics, the studied samples lie in the upper-right portion of the map, highlighting their excellent specific strength. Moreover, Figure S1 shows a comparison of the stress–strain curves recorded for the best samples of each batch. It can be observed that, for SiOC with 0 and ≈11 Vol% SiC, once the maximum stress is reached, the strength drops quite rapidly. In contrast, for the other two batches with higher SiC contents, the strength decreases more gradually, suggesting a possible increase in toughness induced by the presence of SiC particles.

4 | Discussion

The studied process for 3D manufacturing of CCSs with SiC/SiOC(N) composite struts begins with the preparation of a SiC/TPU composite filament. To this end, TPU was compounded with 15 wt%, 20 wt%, and 25 wt% of 2 μm SiC powders, and the resulting compound was extruded into filaments with a diameter of ~1.75 mm. The obtained filaments were mechanically characterized by measuring the elastic modulus, maximum tensile stress, and elongation at break (Table 1). The data show that the initial addition of 15 wt% SiC led to a decrease in elastic modulus, accompanied by an increase in tensile strength and elongation at break. Only when the SiC content was increased beyond 15 wt% (i.e., at 20 wt% and 25 wt%), the elastic modulus of the filaments increased, while the tensile strength decreased. The elongation at break did not show appreciable changes.

Since the Young's modulus of SiC is much higher than that of TPU (E_{TPU} ~ 15 MPa vs. E_{SiC} ~ 300 GPa), a steady increase in elastic modulus with SiC content would have been expected. Instead, the first addition of SiC (15 wt%, which corresponds to 10.3 Vol%, see Table 3) resulted in a reduction of the elastic modulus. This behavior can be explained by assuming that the 2 μm SiC particles dispersed in the TPU matrix exert a twofold effect. On the one hand, they act as a softening agent for the hard domains of TPU, increasing the free volume and the mobility of the polymer chains. This, in turn, leads to an increase in the elongation at break and a decrease in the elastic modulus (see Table 1). On the other hand, the SiC particles act as a stiffening phase, and this effect becomes predominant at higher filler contents (≥ 20 wt%, corresponding to ≥ 15.4 Vol%; see Table 3). Accordingly, when the SiC content exceeded 15 wt%, the stiffness began to increase. This interpretation is consistent with the structure of TPU, which is composed of soft and hard segments [15], also described as flexible and rigid segments [16]. In the latter work, the authors reported an initial increase in the soft-segment fraction upon the addition of SiC to PU at a volume fraction of 0.09, followed by a subsequent decrease.

The 3D-printed SiC/TPU composite cellular structures were impregnated with a Durazane solution, and the corresponding weight and volume increases were measured (Table 2 and Figure 2). Interestingly, the evolution of these two variables with SiC content mirrors the trend observed in the elastic modulus of the polymeric filaments: swelling and Durazane uptake initially

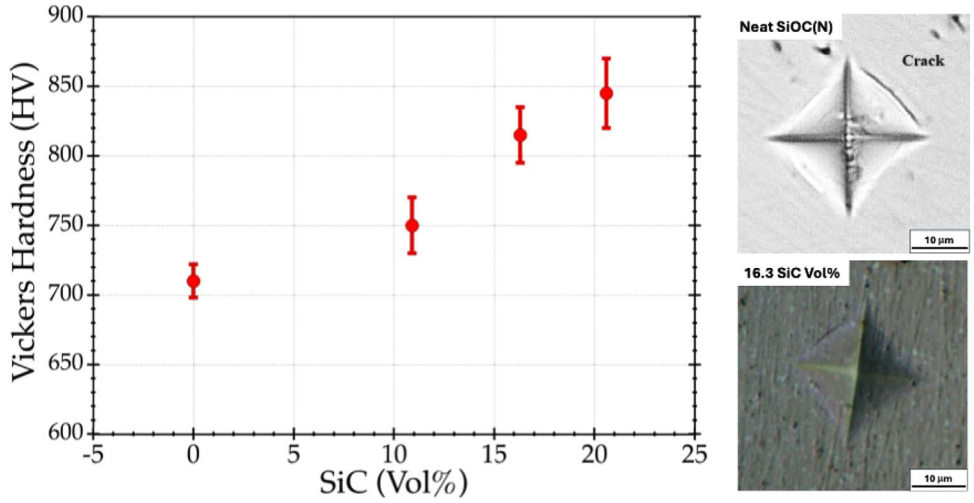

FIGURE 7 | Plot of the Vickers hardness measured on the different composite sample and indentation impressions of the 0 and 16.3 Vol% SiC composites. The cone-like cracks are indicated in the pictures.

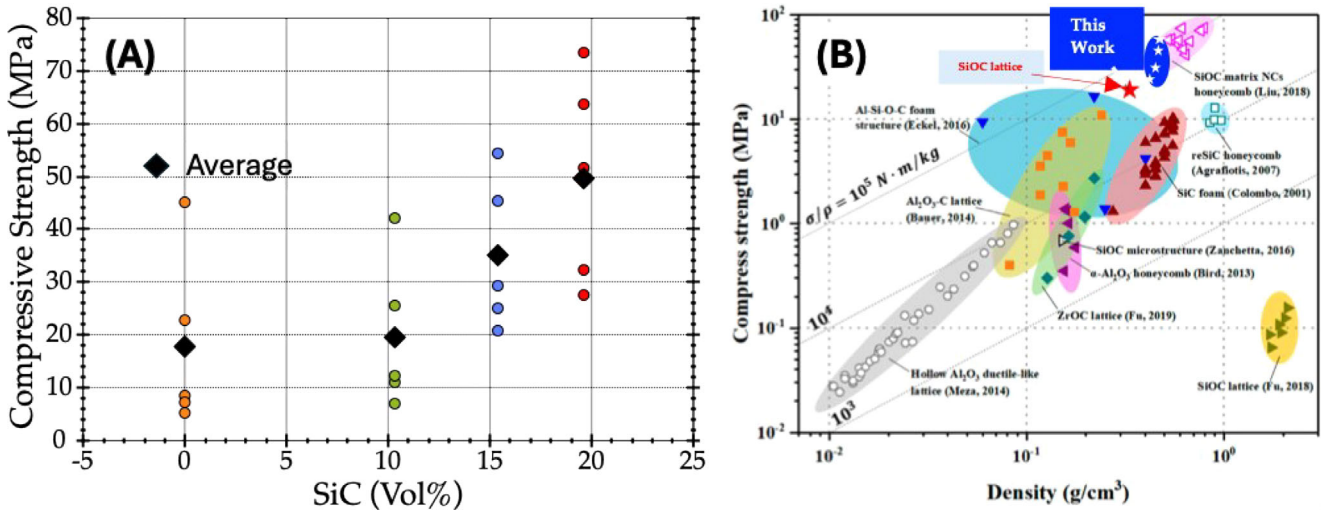

FIGURE 8 | (A) Compressive stress as a function of SiC volume fraction in SiC/SiOC composites pyrolyzed at 1200°C and (B) Ashby chart of compressive strength versus density, referenced from [14].

increase, but both decrease as the SiC content continues to rise.

It is important to note that the TPU matrix, rather than the SiC particles, is responsible for interaction with Durazane through the incorporation of polysilazane molecules between its polymer chains, which results in a mass uptake and a volume swelling.

Therefore, considering that, by increasing the SiC volume fraction, the TPU volume fraction is decreasing, a monotonic decrease in mass uptake and volume swelling with increasing SiC content would have been expected. In other words, no maximum at 15 wt% SiC was anticipated.

This experimental observation can be rationalized by the same argument as before: SiC particles exert a dual effect. On the one hand, they interact with the hard segment of TPU with a resulting softening effect, enabling greater uptake of Durazane. On the other hand, as the SiC content increases further, the relative amount of TPU—the active phase that can host Durazane—decreases, leading to an overall reduction in both mass uptake and volume expansion.

The materials obtained after pyrolysis are ceramic-matrix composites reinforced with a well-dispersed SiC filler. The addition of the filler substantially impacts the physical and mechanical properties of the composite. Specifically, we show that the SiC addition produces a remarkable increase in the compressive strength and hardness of the material, while the density follows the rule of mixture.

The compressive strength can be considered particularly remarkable. In fact, the obtained cellular structures lie on the top part of the Ashby plot (see Figure 8B), correlating compressive strength and geometrical density. It is worth stressing that the material's performance increases with the SiC Vol% (Figure 8A) but also in the strength-density plane increases with the SiC content in the

composite (Figure 8B) showing an excellent specific strength. The overall results point out that the PDC-based replica method can be coupled with FFF to obtain ceramic matrix composites with engineered properties. This opens a new approach to manufacturing ceramic matrix composites with simple and inexpensive printers and reagents, surpassing some limitations of the more diffuse stereolithographic methods.

5 | Conclusion

This work has demonstrated the feasibility of processing composite SiC/SiOC(N) ceramic cellular structures via the replica method, starting from a SiC/TPU composite structure that is first impregnated with a polysilazane and then pyrolyzed in an inert atmosphere. The struts of the resulting ceramic cellular structures are dense, exhibiting a homogeneous distribution of SiC reinforcing particles that reflects the uniform dispersion present in the initial SiC/TPU filament. Composite SiC/SiOC(N) materials containing approximately 11Vol%–21 Vol% SiC were obtained. The skeletal density, hardness, and compressive strength all increase with the amount of SiC reinforcing phase. Finally, this new process is not limited to SiC as a reinforcing agent but can, in principle, be extended to other ceramic or metallic phases, such as TiO_2, Al_2O_3, $MoSi_2$, BN, Si, or Ti, among others. Accordingly, this approach is expected to enable the fabrication of cellular structures with composite ceramic struts whose functional and structural properties can be tailored by the choice of reinforcing phase.

Acknowledgments

Gian Domenico Sorarù and Rajat Chaudhary acknowledge the financial support of Fondazione Cassa di Risparmio di Trento e Rovereto (Grant Number 2021.0569).

Open access publishing facilitated by Universita degli Studi di Trento, as part of the Wiley - CRUI-CARE agreement.

References

1. J. W. Halloran, "Ceramic Stereolithography: Additive Manufacturing for Ceramics by Photopolymerization," *Annual Review of Materials Research* 46, no. 1 (2016): 19–40, https://doi.org/10.1146/annurev-matsci-070115-031841.

2. X. Zhang, K. Zhang, L. Zhang, W. Wang, Y. Li, and R. He, "Additive Manufacturing of Cellular Ceramic Structures: From Structure to Structure–Function Integration," *Materials and Design* 215 (2022): 110470, https://doi.org/10.1016/j.matdes.2022.110470.

3. R. P. Chaudhary, C. Parameswaran, M. Idrees, et al., "Additive Manufacturing of Polymer-Derived Ceramics: Materials, Technologies, Properties and Potential Applications," *Progress in Materials Science* 128 (2022): 100969, https://doi.org/10.1016/j.pmatsci.2022.100969.

4. Z. C. Eckel, C. Zhou, J. H. Martin, A. J. Jacobsen, W. B. Carter, and T. A. Schaedler, "Additive Manufacturing of Polymer-Derived Ceramics," *Science* 351 (2016): 58–62, https://doi.org/10.1126/science.aad2688.

5. P. Colombo, J. Schmidt, G. Franchin, A. Zocca, and J. Günster, "Additive Manufacturing Techniques for Fabricating Complex Ceramic Components From Preceramic Polymers," *American Ceramic Society Bulletin* 96 (2017): 16–23.

6. A. Kulkarni, J. Pearce, Y. Yang, A. Motta, and G. D. Sorarù, "SiOC(N) Cellular Structures With Dense Struts by Integrating Fused Filament Fabrication 3D Printing With Polymer-Derived Ceramics," *Advanced Engineering Materials* 23 (2021), https://doi.org/10.1002/adem.202100535.

7. R. Chaudhary, F. Agostinacchio, R. Canteri, M. Biesuz, A. Motta, and G. D. Sorarù, "Fabrication and Characterization of SiOC(N) Cellular Structures via 3D-Printed Polyurethane Templates Impregnated With Polysilazane," *Journal of the European Ceramic Society* 45 (2025): 117706, https://doi.org/10.1016/j.jeurceramsoc.2025.117706.

8. Y. Yang, A. Kulkarni, G. D. Soraru, J. M. Pearce, and A. Motta, "3D Printed SiOC(N) Ceramic Scaffolds for Bone Tissue Regeneration: Improved Osteogenic Differentiation of Human Bone Marrow-Derived Mesenchymal Stem Cells," *International Journal of Molecular Sciences* 22 (2021): 13676, https://doi.org/10.3390/ijms222413676.

9. Q. Han, J. Zhang, H. Chen, et al., "The Effect of Graphitization Degree of Carbon and Si—O—C Network on the Electrochemical Performance of SiOC Anodes," *International Journal of Applied Ceramic Technology* 21 (2024): 2332–2341, https://doi.org/10.1111/ijac.14625.

10. X. Lin, S. Sui, S. Tan, C. U. Pittman, J. Sun, and Z. Zhang, "Fast Pyrolysis of Four Lignins From Different Isolation Processes Using Py-GC/MS," *Energies* 8 (2015): 5107–5121., https://doi.org/10.3390/en8065107.

11. V. Siipola, T. Tamminen, A. Källi, et al., "Effects of Biomass Type, Carbonization Process, and Activation Method on the Properties of Bio-Based Activated Carbons," *BioResources* 13 (2019): 5976–6002, https://doi.org/10.15376/biores.13.3.5976-6002.

12. C. Moysan, R. Riedel, R. Harshe, T. Rouxel, and F. Augereau, "Mechanical Characterization of a Polysiloxane-Derived SiOC Glass," *Journal of the European Ceramic Society* 27 (2007): 397–403, https://doi.org/10.1016/j.jeurceramsoc.2006.01.016.

13. T. Rouxel, J.-C. Sanglebœuf, J.-P. Guin, V. Keryvin, and G.-D. Soraru, "Surface Damage Resistance of Gel-Derived Oxycarbide Glasses: Hardness, Toughness, and Scratchability," *Journal of the American Ceramic Society* 84 (2004): 2220–2224, https://doi.org/10.1111/j.1151-2916.2001.tb00991.x.

14. Z. Li, Z. Chen, J. Liu, et al., "Additive Manufacturing of Lightweight and High-strength Polymer-derived SiOC Ceramics," *Virtual and Physical Prototyping* 15 (2020): 163–177, https://doi.org/10.1080/17452759.2019.1710919.

15. J. G. Drobny, "9 Thermoplastic Polyurethane Elastomers," in *Handbook Thermoplastic Elastomers*, 2nd ed. (Springer, 2014), 233–253, https://doi.org/10.1016/B978-0-323-22136-8.00009-0.

16. T. A. Shalygina, M. S. Rudenko, I. V. Nemtsev, et al., "Influence of the Filler Particles' Surface Morphology on the Polyurethane Matrix's Structure Formation in the Composite," *Polymers* 13, no. 22 (2021): 3864, https://doi.org/10.3390/polym13223864.

Supporting Information

Additional supporting information can be found online in the Supporting Information section.

Supporting File 1: jace70635-sup-0001-SuppMat.docx.